

Dependence of the Transmission Characteristics of Photonic Crystal Fiber on the Macrobending Radius and the Mechanically Induced Microbending

Dae Seung Moon, Joo Beom Eom, Jinchae Kim, Hokyoung Kim, Byeong Ha Lee*, and Un-Chul Paek

*Department of Information and Communications Kwangju Institute of Science and Technology,
Gwangju 500-712, KOREA*

(Received March 27, 2003)

It is reported that the spectral loss of photonic crystal fiber (PCF) having a large hole-to-hole distance ($\sim 10 \mu\text{m}$) is sensitive to micro- and macrobending when compared with the conventional single-mode fiber. In this paper, we will present the measurement result of the macro- and microbending characteristics of fabricated PCF with large hole-to-hole distance ($> 10 \mu\text{m}$). For the macrobending experiment, the fiber was simply wound around a circular structure with variable diameter that could be reduced to a few centimeters. For the microbending case, regularly spaced silica rods were attached on a slide glass and pressed against the fiber by loading a stack of metal plates of known weight on the glass. The transmission loss spectrum shows a rather flat response to the to microbending, and this makes the PCF a good candidate for a wideband variable optical attenuator.

OCIS codes : 060.2400, 060.2370, 060.2270.

I. INTRODUCTION

Unlike the standard optical fiber whose core and cladding are made of different materials, the photonic crystal fiber (PCF), also known as holey fiber, is usually made of a single material with many air holes. The PCF is fabricated by introducing a defect or a missing air hole in an array of regularly spaced tiny air holes running along the propagation axis, and the light is guided along the defect. Its unique characteristics include the single-mode operation in a wide wavelength range [1], tailorable dispersion, nonlinear properties [2]- [6], large mode field diameter [7], grating resonances [8], and birefringence [9]. These properties are potentially very useful for making novel fiber devices such as dispersion-managed fibers, fiber gratings, nonlinear fiber and fiber sensors. By modifying the structure of the air holes, we can make PCF with unusual optical properties. There are two different mechanisms employed to explain the light guiding through PCF; one is the effective index guiding [1,2], also referred to as modified total internal reflection, and the other is photonic bandgap guiding [10,11]. Most of the experimental results reported so far have been explained by the effective index guiding because

photonic bandgap guiding requires a strictly periodic array of large air holes, which is difficult to fabricate. Fabrication of PCF is rather different from that of standard optical fiber because of the many air holes in the cladding region. Thus a special fabrication technique such as high-tension drawing is required [12].

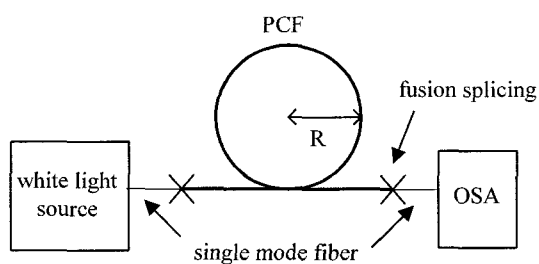
In general, compared with the conventional single mode fiber (SMF), the PCF with large hole-to-hole distance is much more sensitive to bending. In this paper, the micro- and macrobending effects on the fabricated PCF with a large hole-to-hole distance ($\sim 10 \mu\text{m}$) will be presented.

II. MACROBENDING CHARACTERISTICS OF PCF

In order to measure the macrobending characteristics of PCF, a white-light source (Ando AQ4303B) and an OSA (Ando AQ6317B) were used. Fig. 1(a) shows the scanning electron microscope image of the cross-section of the PCF fabricated for the experiment. The fabricated PCF had $11.9 \mu\text{m}$ hole-to-hole distance, and the hole diameter and outer diameter were $4.4 \mu\text{m}$ and $140 \mu\text{m}$, respectively. Fig. 1(b) shows the ex-



(a)



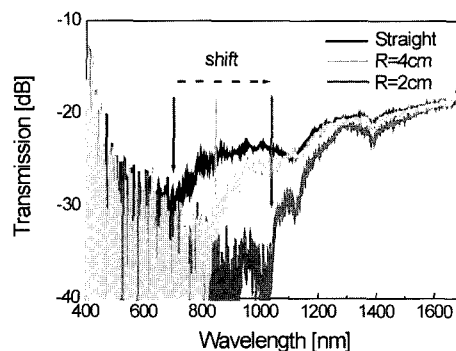
(b)

FIG. 1. (a) The cross-sectional image of the PCF used for the experiment on the macrobending effect. (b) The experimental setup for measuring the macrobending characteristics of the PCF.

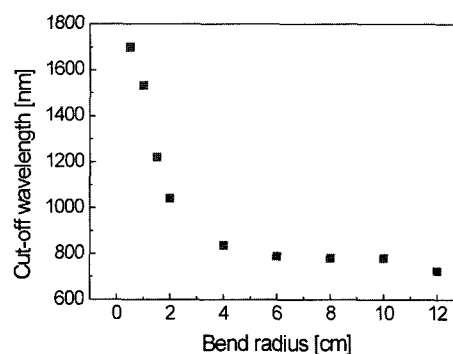
perimental setup used for measuring the macrobending characteristics of the PCF. Both ends of the PCF were connected to single-mode fibers. The length of the PCF used for the experiment was about 87 cm.

The measurement of the macrobending characteristics of PCF was done by the single-turn radius method. Fig. 2(a) shows the measured transmission spectra of the straight PCF and the PCF with the bending radii of 2 cm and 4 cm. In the case of the straight PCF, the cutoff wavelength was about 700 nm, which increased as the bending radius decreased. The cutoff wavelengths were 830 nm and 1040 nm for bending radii of 4 cm and 2 cm, respectively.

Fig. 2(a) shows that the cutoff wavelength of the mode shifts to the longer wavelength as the bending radius decreases. This means the macrobending limits the light propagation in the PCF at shorter wavelength. We define the critical bending radius as the radius at which the cutoff wavelength just begins to increase. Fig. 2(b) shows the variation of the cutoff wavelength with the bending radius and the critical bending radius was measured to be 12 cm. The critical bending radius mainly depends on the structure of the PCF, such as the hole-to-hole distance, the hole diameter, and the wavelength [1]. The critical bend-



(a)



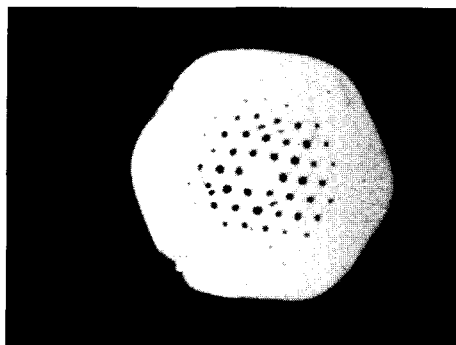
(b)

FIG. 2. (a) The transmission spectra of the PCF in terms of the bending radius. (b) The cutoff wavelength changes of the PCF with respect to the bending radius.

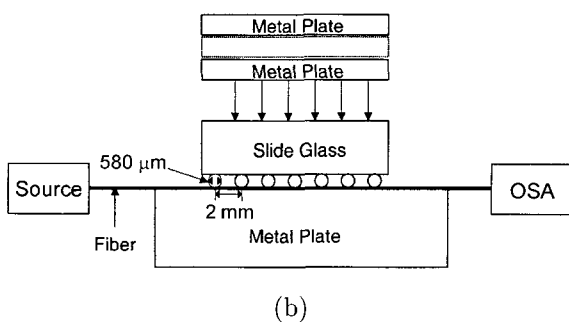
ing radius is larger for larger hole-to-hole distance and shorter wavelength [1].

III. MICROBENDING CHARACTERISTICS OF PCF

It is known that the PCF with large hole-to-hole distance is more sensitive to bending in general. In addition, the sensitivity also depends on other parameters such as the dimensions of the holes and the wavelength. In the case of SMF, microbending effects have been widely investigated [14]- [16]. However, in the case of PCF, even though macrobending has been investigated [1,13], the microbending of the PCF is still being researched. In this section, the microbending effect on the PCF for various experimental conditions, such as the periodicity and the radius of the microbending-inducing rods, will be presented.



(a)



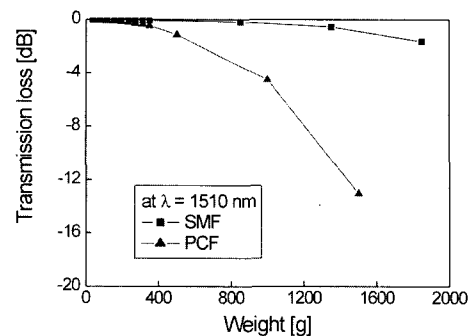
(b)

FIG. 3. (a) The cross-sectional image of the PCF used in the experiment on the microbending effect. The outer diameter is $120 \mu\text{m}$. (b) The experimental setup for measuring the microbending characteristics of the PCF and the SMF.

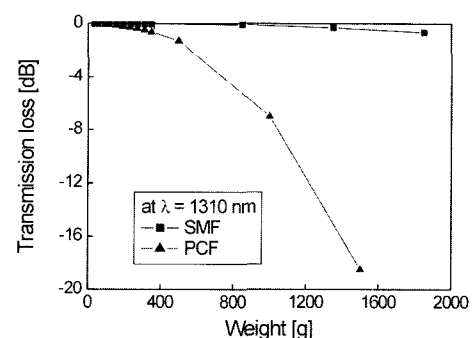
1. The Comparison of Microbending Effects on PCF and SMF

In this subsection, we will make a comparison of the effect of microbending on PCF and SMF. Fig. 3(a) shows the microscope image of the cross-section of the PCF used in the experiment. Its hole-to-hole distance was $10.8 \mu\text{m}$, and the air hole diameter and outer diameter were $5.1 \mu\text{m}$ and $120 \mu\text{m}$, respectively. Fig. 3(b) shows the experimental setup used for measuring the microbending characteristics of the PCF and the SMF.

For the microbending study, a bundle of regularly spaced silica rods were attached on a slide glass and pressed against the polymer-coated fibers (PCF or SMF) by loading a stack of metal plates ($50 \text{ mm} \times 75 \text{ mm}$) of known weight. The silica rods were obtained by the drawing process. With this scheme, it was possible to study the effect of periodic microbending by varying the number and the diameter of silica rods and the weight of the load. The silica rods had the



(a)



(b)

FIG. 4. The variation of the transmission loss of the PCF and SMF measured at the wavelengths of (a) 1310 nm and (b) 1510 nm.

approximately equal diameter of about $580 \mu\text{m}$ and spaced by an interval of 2 mm. The total length of the microbend-inducing region was about 5 cm. Figs. 4(a) and (b) show the variation of the transmission loss of the PCF and the SMF measured at the wavelengths of 1310 nm and 1510 nm, respectively. Both figures show that the attenuation is proportional to the weight and that PCF is more sensitive than SMF. In the case of the PCF, unlike the SMF, the spectral change was more sensitive to the microbending in the short wavelength region than in the long wavelength region. The data clearly shows higher sensitivity of the PCF to microbending than the SMF, which makes the PCF with larger hole size more suitable for pressure sensing applications.

Fig. 5 shows the transmission spectra of the PCF under microbending, which shows rather flat transmission spectra over a wide wavelength range. It also shows that the spectra remain nearly flat even with microbending applied. These data indicate that it is possible to fabricate wideband variable optical attenuators using PCF.

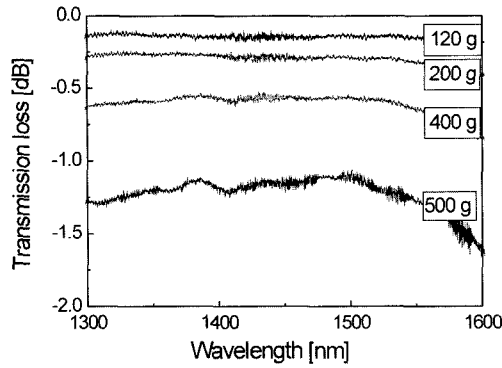


FIG. 5. The transmission spectra of microbending induced PCF.

2. Dependence of the PCF Transmission Characteristics on the Length of Microbend-Inducing Region

In this subsection, we will describe the dependence of the transmission characteristics of PCF on the length of microbend-inducing region by increasing the number of silica rods with the same radius as shown in Fig. 6(a). The diameter of each rod was $450\ \mu\text{m}$. We considered two configurations with 18 and 36 silica rods, which provided microbending regions of 0.8 cm and 1.6 cm, respectively. There was no gap between

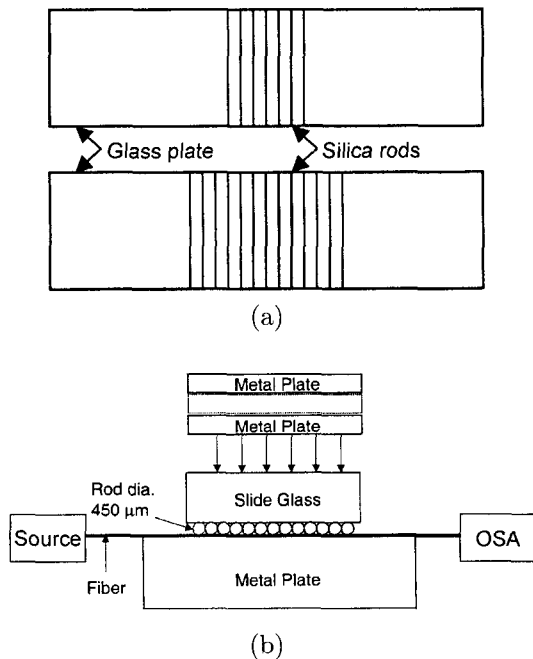


FIG. 6. (a) The schematic of the configuration used to change the length of the microbend-inducing region. (b) The experimental setup.

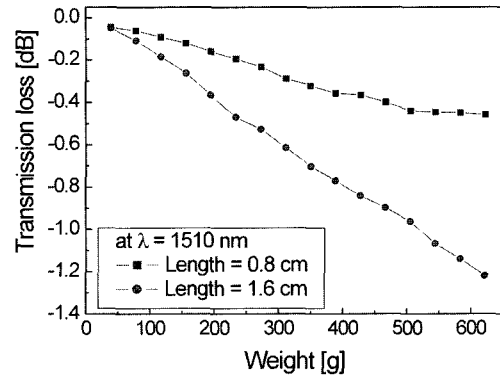


FIG. 7. The variation of transmission loss of PCF for two different lengths of the microbend-inducing region with the period of $450\ \mu\text{m}$.

the rods. Fig. 6(b) shows the experimental setup. The PCF used for the experiment had $10.4\ \mu\text{m}$ hole-to-hole distance, $4.7\ \mu\text{m}$ diameter air hole, and $125\ \mu\text{m}$ outer diameter. Fig. 7 shows the variation of the transmission loss for the two configurations. The sensitivity increases with the length of the microbend-inducing region. In other words, as the number of rods increased, the number of corrugations on the surface of the PCF also increased, which leads to more attenuation as expected.

3. Dependence of the PCF Transmission Characteristics on the Microbending Period

In this subsection, measurement of the effect of microbending on the PCF characteristics using small silica rods will be described. The microbending period was changed by varying the diameter of the silica rods. The diameter and the number of silica rods in two different configurations were chosen so as to maintain approximately the same length of the total microbend-inducing region, i.e., $580\ \mu\text{m} \times 24\ \text{pieces} \sim 1.39\ \text{cm}$ and $420\ \mu\text{m} \times 33\ \text{pieces} \sim 1.39\ \text{cm}$. Figs. 8(a) and (b) show the schematic of the two configurations and the experimental setup, respectively. Figs. 9(a) and (b) show the transmission loss of the PCF measured at the wavelength of $1310\ \text{nm}$ and $1510\ \text{nm}$, respectively. From Figs. 9(a) and (b), it is seen that larger microbending period results in more transmission loss. When the pressure is applied on the PCF by the periodic microbending, the local radius of periodic corrugations will be larger for larger period. In the case of microbending, unlike the macrobending case [13], the transmission loss increased as the diameter of the silica rod in the microbend-inducing region increased.

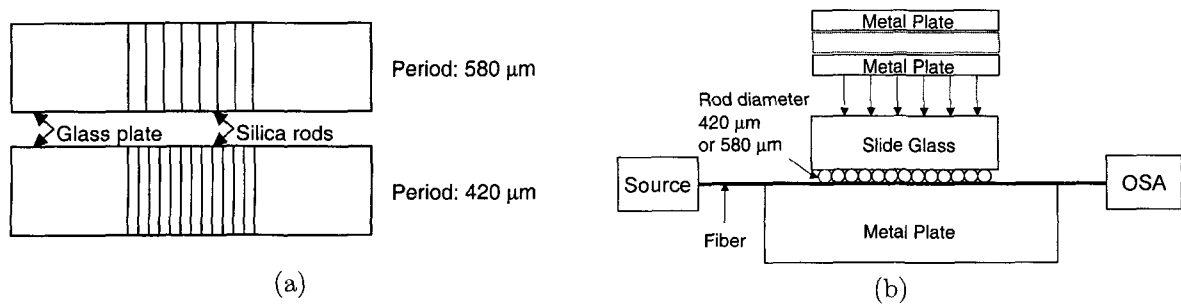


FIG. 8. (a) The schematic of the configuration used to increase the period of microbend while maintaining the length of the microbend-inducing region. (b) The experimental setup.

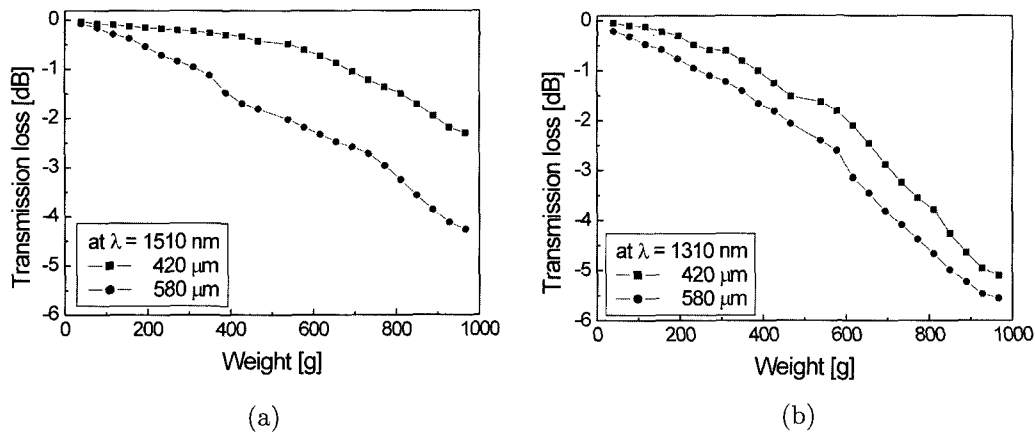


FIG. 9. The variation of the transmission loss of the PCF due to the microbending with $420 \mu\text{m} / 580 \mu\text{m}$ period measured at the wavelengths of (a) 1310 nm and (b) 1510 nm .

Figs. 10(a) and (b) show the transmission loss of the PCF by the microbending with the periods of $420 \mu\text{m}$ and $580 \mu\text{m}$, respectively.

In Figs. 10(a) and (b), it is seen that the PCF is more sensitive to microbending at short wavelength. This phenomenon can be explained in terms of the

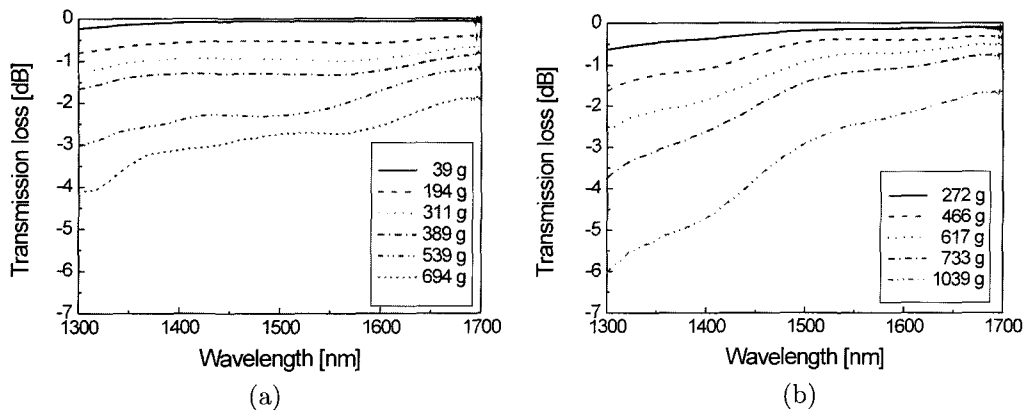


FIG. 10. The transmission loss spectra of the PCF induced by microbending with the periods of (a) $420 \mu\text{m}$ and (b) $580 \mu\text{m}$.

mode confinement in PCF. At short wavelength, the field is mainly confined to the silica region, whereas at longer wavelength a relatively large portion of the field can penetrate to the air holes near the central defect. Thus, the effective cladding index of the PCF at long wavelength is lower than that at short wavelength. This implies that the refractive index difference between the silica and the effective cladding decreases with decreasing wavelength and that the field confinement of the guided mode decreases as well. This causes the unusual property of large bending loss at short wavelength in the PCF [13].

IV. CONCLUSION

In this work, we presented the measurement results of the transmission characteristics of PCF subjected to micro- and macrobending. We found that the PCF was rather sensitive to the bending effect compared to the conventional single-mode fiber. This is due to the presence of the regularly spaced air holes running in the direction of the light propagation.

In the case of macrobending, the transmission spectra of the PCF were measured using the single-turn bend radius method. The cutoff wavelength of the mode shifted to the long wavelength when the bend radius was decreased. This implies that the macrobending effect limits the light propagation in the PCF in the short wavelength range. For measurements of the microbending effect, we used silica rods of identical dimension attached to a glass slide. The microbending effect was then induced in the PCF by pressing the glass slide with known weight. Using this configuration, we measured the dependence of the PCF transmission characteristics on the microbending period and the length of microbend-inducing region by varying the diameter and the number of the silica rods and the spacing between them. The transmission loss of the PCF clearly shows the higher sensitivity of the PCF to the load weight when compared with the SMF, which can make PCF a good candidate for pressure sensing head. The transmission loss of the PCF was also found to increase as the length of microbend-inducing region was increased. In contrast to the case of macrobending where the loss was smaller for larger bending radius, the transmission was more lossy when the diameter of rods was larger, i.e., when the local radius of the corrugation was larger.

The sensitivity to microbending was higher in the short wavelength region than in the long wavelength region. It is possible to have a relatively flat transmission loss by choosing appropriate diameter of the silica rods, and since the flatness is maintained even if the weight is increased, PCF has a good potential as a wideband variable optical attenuator.

ACKNOWLEDGEMENTS

This work was partially supported by KISTEP through Critical Technology 21 Program and BK-21 Program of MOE, Korea.

*Corresponding author : leebh@kjist.ac.kr.

REFERENCES

- [1] J. C. Knight, T. A. Birks, and P. St. J. Russell, "Endlessly single-mode photonic crystal fiber," *Opt. Lett.*, vol. 22, no. 13, pp. 961-963, 1997.
- [2] T. A. Birks, D. Mogilevtsev, J. C. Knight, and P. St. J. Russell, "Dispersion compensation using single-material fibers," *IEEE Photon. Technol. Lett.*, vol. 11, no. 6, pp. 674-676, 1999.
- [3] M. J. Gander, R. McBride, J. D. C. Jones, D. Mogilevtsev, T. A. Birks, J. C. Knight, and P. St. J. Russell, "Experimental measurement of group velocity dispersion in photonic crystal fiber," *Electron. Lett.*, vol. 35, no. 1, pp. 63-64, 1999.
- [4] W. J. Wadsworth, J. C. Knight, A. Ortigosa-Blanch, J. Arriaga, E. Silvestre, and P. St. J. Russell, "Soliton effects in photonic crystal fibres at 850 nm," *Electron. Lett.*, vol. 36, no. 1, pp. 53-55, 2000.
- [5] N. G. R. Broderick, T. M. Monro, P. J. Bennett, and D. J. Richardson, "Nonlinearity in holey optical fibers: Measurement and future opportunities," *Opt. Lett.*, vol. 24, no. 20, pp. 1395-1397, 1999; errata on 15 Nov. 1999.
- [6] D. Mogilevtsev, T. A. Birks, and P. St. J. Russell, "Group-velocity dispersion in photonic crystal fibers," *Opt. Lett.*, vol. 23, no. 21, pp. 1662-1664, 1999.
- [7] J. C. Knight, T. A. Birks, R. F. Cregan, P. St. J. Russell, and J. P. de Sandro, "Large mode area photonic crystal fibre," *Electron. Lett.*, vol. 34, no. 14, pp. 1347-1348, 1998.
- [8] B. J. Eggleton, P. S. Westbrook, C. A. White, C. Kerbage, R. S. Windeler, and G. L. Burdge, "Cladding-mode-resonances in air-silica microstructure optical fiber," *J. Lightwave Technol.*, vol. 18, no. 8, pp. 1084-1100, 2000.
- [9] A. Ortigosa-Blanch, J. C. Knight, W. J. Wadsworth, J. Arriaga, B. J. Mangan, T. A. Birks, and P. St. J. Russell, "Highly birefringent photonic crystal fibers," *Opt. Lett.*, vol. 25, no. 18, pp. 1325-1327, 2000.
- [10] E. Yablonovitch, "photonic band-gap structures," *J. Opt. Soc. Am. B*, vol. 10, no. 2, pp. 283-295, 1993.
- [11] J. C. Knight, J. Broeng, T. A. Birks, and P. St. J. Russell, "Photonic band gap guidance in optical fibers," *Science*, vol. 282, pp. 1476-1479, 1998.
- [12] J. B. Eom, K. W. Park, T. -J. Eom, Y. Chung, W. -T. Han, U. C. Paek, and B. H. Lee, "Transmission and numerical aperture measurement of photonic crystal fiber," in *OECC 2001*, OSA, Sydney, Postdeadline, PDP 2.05, 2001.
- [13] T. Sorensen, J. Broeng, A. Bjarklev, E. Kundsén, and E. E. Barkou Libori, "Macro-bending loss properties

- of photonic crystal fibre," *Electron. Lett.*, vol.37, no.5, pp. 287-288, 2001.
- [14] D. Marcuse, "Microdeformation losses of single-mode fibers," *Appl. Opt.*, vol. 23, no. 7, pp. 1082-1091, 1984.
- [15] H. F. Taylor, "Bending effects in optical fibers." *J. Lightwave Technol.*, vol. LT-2, no. 5, pp. 617-628, 1984.
- [16] K. Petermann, and R. Kuhne, "Upper and lower limits for the microbending loss in arbitrary single-mode fibers," *J. Lightwave Technol.*, vol. LT-4, no. 1, pp. 2-7, 1986.